Dynamic Measurement of the pH of the Golgi Complex in Living Cells Using Retrograde Transport of the Verotoxin Receptor

Jae Hong Kim,*§‖ Clifford A. Lingwood,‡¶‡‡ David B. Williams,** Wendy Furuya,§ Morris F. Manolson,§** and Sergio Grinstein§****

Divisions of *Gastroenterology and Nutrition, ‡Microbiology, and §Cell Biology, Research Institute, Hospital for Sick Children; ‖Institute of Medical Science; and Departments of ¶Microbiology, **Biochemistry, and ‡‡Clinical Biochemistry, University of Toronto, Toronto, Ontario, Canada

Abstract. The B subunit of verotoxin (VT1B) from enterohemorrhagic *Escherichia coli* is responsible for the attachment of the holotoxin to the cell surface, by binding to the glycolipid, globotriaosyl ceramide. After receptor-mediated endocytosis, the toxin is targeted to the Golgi complex by a process of retrograde transport. We took advantage of this unique property of VT1B to measure the pH of the Golgi complex in intact live cells. Purified recombinant VT1B was labeled with either rhodamine or fluorescein for subcellular localization by confocal microscopy. After 1 h at 37°C, VT1B accumulated in a juxtanuclear structure that colocalized with several Golgi markers, including α-mannosidase II, β-COP, and NBD-ceramide. Moreover, colchicine and brefeldin A induced dispersal of the juxtanuclear staining, consistent with accumulation of VT1B in the Golgi complex. Imaging of the emission of fluorescein-labeled VT1B was used to measure intra-Golgi pH (pH_G), which was calibrated in situ with ionophores. In intact Vero cells, pH_G averaged 6.45 ± 0.03 (standard error). The acidity of the Golgi lumen dissipated rapidly upon addition of bafilomycin A_1, a blocker of vacuolar-type ATPases. pH_G remained constant despite acidification of the cytosol by reversal of the plasmalemmal Na^+/H^+ antiport. Similarly, pH_G was unaffected by acute changes in cytosolic calcium. Furthermore, pH_G recovered quickly toward the basal level after departures imposed with weak bases. These findings suggest that pH_G is actively regulated, despite the presence of a sizable H^+ "leak" pathway. The ability of VT1B to target the Golgi complex should facilitate not only studies of acid-base regulation, but also analysis of other ionic species.

THE secretory pathway is composed of an elaborate network of cisternal, tubulo-vesicular, and vesicular compartments comprising the ER, Golgi apparatus, and transport and secretory vesicles (Mellman and Simons, 1992). While the enzymatic and processing components of the biosynthetic pathway have been studied extensively, comparatively little is known about the ionic composition of these compartments. Of particular interest is the luminal pH, which is thought to play an important role in posttranslational processing and packaging of proteins, as well as in the formation and traffic of vesicles (Yilla et al., 1993; Mellman et al., 1986). The distal compartments of the secretory pathway are thought to be acidic, and maintenance of a reduced pH is believed to be essential for normal function. These conclusions were initially inferred from the detection of vacuolar-type (V)[1] ATPases in purified secretory granules and Golgi membranes (Glickman et al., 1983) and from the use of protonophores and permeant weak bases, which were found to interfere with proper protein and lipid synthesis and sorting (Tartakoff, 1983*a*). More direct evidence for the existence of a pH gradient across membranes of the late secretory pathway was provided by Anderson et al. (1984) using 3-(2,4-dinitroanilino)-3′-amino-*N*-methyl-dipropylamine (DAMP), a weak base that partitions preferentially into acidic organelles and can be fixed and detected microscopically. This elegant approach, however, is not applicable to living cells and has limited quantitative resolution. Thus, the information regarding the pH of secretory or-

Address all correspondence to Sergio Grinstein, Division of Cell Biology, Hospital for Sick Children, 555 University Avenue, Toronto M5G 1X8, Canada. Tel.: (416) 813-5727. Fax: (416) 813-5028.

1. *Abbreviations used in this paper*: BCECF, 2′, 7′-bis(carboxyethyl)-carboxylfluorescein; C_5-DMB-ceramide, *N*-[5-(5,7-dimethyl BODIPY)-1-pentanoyl]-D-erythro-sphingosine; DAMP, 3-(2,4-dinitroanilino)-3′-amino-*N*-methyl-dipropylamine; Endo H, endoglycosidase H; MHC, major histocompatibility complex; RITC, rhodamine isothiocyanate; V, vacuolar-type; VT1, verotoxin 1.

ganelles and its dynamic regulation is rather limited, largely due to the lack of suitably targeted analytical methods.

By contrast, the ionic composition and pH of the endocytic pathway have been studied in great detail, using primarily fluorescent probes (Ohkuma and Poole, 1978; Tycko and Maxfield, 1982; Yamashiro et al., 1983). These can be delivered to specific compartments along the endocytic pathway by coupling to receptor ligands or by pulsing the medium with labeled fluid-phase markers, followed by chasing for the appropriate times (Galloway et al., 1983; Geisow, 1984). Using these procedures in combination with modern imaging techniques, it has been possible to monitor continuously and in a noninvasive manner the ionic activity of individual endocytic organelles in viable cells. Thus far, comparable studies have not been performed for the secretory pathway, as it is not readily accessible in intact cells.

This study describes a procedure for targeting the Golgi apparatus of intact viable cells with pH -sensitive fluorescent probes. We took advantage of the endogenous retrograde pathway of mammalian cells to deliver verotoxin 1 (VT1) to the Golgi complex (Sandvig et al., 1992). Like the closely related Shiga toxin, VT1 is a multimeric protein consisting of a single A subunit responsible for inhibition of protein synthesis and five identical B subunits that bind to cellular receptors. VT1 recognizes the glycolipid, globotriaosyl ceramide (Gb_3) on the plasma membrane of susceptible cells and is subsequently internalized by receptor-mediated endocytosis and directed to the ER, where the cytotoxic A subunit is thought to enter the cytosol (Tesh and O'Brien, 1988). EM studies have indicated that the toxin transits the Golgi apparatus en route to the ER and nuclear envelope. We hypothesized that, if the residence time of VT1 in the Golgi complex is sufficient, the toxin could be used to monitor the luminal pH of this compartment in single cells. To this end, recombinant B subunit of VT1 was labeled with fluorescein, a pH-sensitive probe, and its fate within the cell was defined by colocalization with markers of subcellular organelles using confocal microscopy. By separating the receptor-binding from the cytotoxic subunits of VT1, we have therefore devised a method for the continuous, noninvasive measurement of Golgi pH in viable cells under physiological conditions.

Materials and Methods

Materials

FITC-labeled dextran, Texas red–labeled transferrin, Con A, WGA, MitoTracker, and *N*-[5-(5,7-dimethyl BODIPY)-1-pentanoyl]-D-erythro-sphingosine (C_5-DMB-ceramide) were purchased from Molecular Probes, Inc. (Eugene, OR) Anti-tubulin antibody was obtained from Sigma Chemical Co. (St. Louis, MO). FITC- and Cy3-labeled donkey anti–rabbit and anti–mouse antibodies were from Jackson ImmunoResearch Laboratories, Inc. (West Grove, PA). mAb to β-COP and α-mannosidase II were kind gifts from Dr. W. Balch (Scripps Research Institute, La Jolla, CA) and Drs. K.W. Moremen and M. Farquhar (University of California at San Diego, CA), respectively. The mAb 10E6 was a kind gift from Dr. W. Brown (Cornell University, Ithaca, NY). α-Methyl-mannoside and *N*-acetylglucosamine were purchased from Aldrich Chemical Co. (Milwaukee, WI).

Toxin Purification, Labeling, and Characterization

Recombinant B subunit of VT1 (Ramotar et al., 1990) was purified as described earlier by affinity chromatography (Boulanger et al., 1994). Purified VT1B was fluoresceinated by the addition of FITC directly to VT1B (1:1 (wt/wt) ratio) in 0.5 M $Na_2CO_3/NaHCO_3$, pH 9.5. The mixture was gently rotated for 1–2 h at room temperature, after which free FITC was removed. Rhodamine isothiocyanate (RITC)–labeled VT1B was similarly prepared. Excitation and emission spectra of the labeled derivatives of VT1B in solution were generated using a fluorescence spectrophotometer (F4000; Hitachi Instruments, Inc., San Jose, CA). The pH of these solutions was altered using small aliquots of 100 mM citric acid to a solution containing 120 mM NaCl, and 20 mM Tris, pH 8.0, and was monitored with a standard combination probe.

Cell Culture

Vero and HeLa cells obtained from the American Type Culture Collection (Rockville, MD) were cultured at 37°C in MEM containing glutamine, vitamins, 5% FCS, 40 μg/ml gentamicin, 20 U/ml penicillin, and 20 mg/ml streptomycin under 5% CO_2. Viability was assessed by exclusion of Trypan blue. Where indicated, the cells were counted electronically using a Coulter counter (Hialeah, FL) after suspension by trypsinization.

Immunocytochemistry and Confocal Microscopy

Vero cells, grown to near-confluence on 18-mm-diam glass coverslips, were washed three times in cold PBS containing 1 mM $CaCl_2$ and 1 mM $MgCl_2$, pH 7.4. To monitor the distribution of FITC-VT1B, the cells were exposed to 10 μg/ml of the appropriately labeled toxin in PBS for 1 h at 4°C to promote binding to the plasmalemmal receptors without endocytosis. Internalization was then initiated by raising the temperature to 37°C for the specified periods. Where noted, the cells were treated with 0.5 mM colchicine or with 5 μg/ml brefeldin A. The cells were immediately fixed in 4% paraformaldehyde in PBS at room temperature for 30 min, washed with 100 mM glycine, and finally permeabilized with 0.1% Triton X-100 in PBS. Using a similar protocol, the distribution of Texas red–labeled transferrin (100 μg/ml) was assessed after warming the cells to 37°C for 30 min. For endosomal labeling, the cells were incubated with 0.75 mg/ml FITC-dextran for 15 min at 37°C, whereas an overnight incubation was used for lysosomal labeling. Fixed, permeabilized cells were stained with Texas red-Con A (2–5 μg/ml) or Texas red-WGA (2–5 μg/ml) by incubation at 37°C for 30 min.

For immunofluorescence, fixed and permeabilized cells were blocked with 5% horse or donkey serum in PBS containing 0.1% BSA and 0.1% Triton X-100 for 20 min at room temperature, washed three times with PBS, and incubated with primary antibody for 2 h in PBS containing 0.1% BSA and 0.1% Triton X-100. The samples were then washed three times with PBS and incubated with secondary antibody for 1 h, also in PBS containing 0.1% BSA and 0.1% Triton X-100. The following dilutions of the antibodies were used: α-mannosidase II, 1:1,000; calnexin, 1:200; β-COP, 1:200; 10E6, 1:500; tubulin, 1:500; FITC- or Cy3-labeled donkey anti–rabbit IgG, 1:500; FITC- or Cy3-labeled donkey anti–mouse, 1:100. After washing three times with PBS, the samples were treated with Slow Fade (Molecular Probes, Inc.) before mounting. Control experiments were performed by omitting the primary antibody. Samples were analyzed using a laser confocal microscope with a ×63 objective (LSM 410; Zeiss, Oberkochen, Germany). Digitized images were cropped in Adobe Photoshop and imported to Adobe Illustrator (Adobe Systems, Inc., Mountain View, CA) for assembly and labeling. We thank Dr. G.P. Downey (University of Toronto, Canada) for allowing us access to the confocal microscope.

Assays of Golgi Function

Lipid export from the Golgi, a measure of secretory activity, was assessed by the procedure of Ktistakis et al. (1995). Vero cells were treated with VT1B as described above, and then incubated with 5 μg/ml C_5-DMB-ceramide for 30 min. After removal of excess ceramide, the cells were chased for 30 min or 24 h at 37°C, washed, trypsinized, and fixed in 1.5% paraformaldehyde before quantitation of fluorescence by flow cytometry.

To assess the effect of VT1B on exocytic protein transport through the Golgi, we monitored the processing of N-linked oligosaccharides on major histocompatibility complex (MHC) class I molecules in HeLa cells. After a 30-min preincubation in cysteine/methionine-free medium, the cells were labeled for 15 min with 100 μCi/ml of [^{35}S]Cys/Met. This was followed by a chase in DME + 10% serum for the indicated periods. Cells were then rinsed in ice-cold PBS, lysed in 1% NP-40 in PBS, pH 7.2, with 1% aprotinin and 2 mg/ml iodoacetamide, and subjected to immunoisola-

tion with 2 μl of anti-MHC class I antibody (W6/32) and protein A–agarose beads. After 1 h at 4°C, the beads were washed four times in 0.5% NP-40, 10 mM Tris, 150 mM NaCl, 1 mM EDTA, and 0.02% NaN_3, pH 7.4. Samples were then heated for 5 min at 70°C in 50 μl of 0.1 M citrate, 0.2% SDS, pH 6.0, and incubated with or without endoglycosidase H (Endo H) for 3 h at 30°C. Samples were analyzed by SDS-PAGE and autoradiography using Amplify (Amersham Corp., Arlington Heights, IL).

Video Imaging

Simultaneous imaging of FITC-VT1B fluorescence and of cell morphology was performed using an inverted microscope (Axiovert I35; Zeiss, Oberkochen, Germany) equipped with epifluorescence optics. Excitation at 440 and 490 nm was provided by a xenon arc lamp via a computer-controlled shutter and filter wheel assembly (Sutter Instrument Co., Novato, CA), while continuous 620-nm illumination was achieved by filtering the transmitted incandescent source. The excitation light was attenuated by a neutral density filter and reflected to the cells by a dichroic mirror (510 nm), while the emitted fluorescence (>510 nm) and the transmitted red light (>620 nm) were separated by an emission dichroic mirror (580 nm). The red light was directed to a video camera, allowing continuous visualization of the cells, while the fluorescent light was directed onto a 542 ± 62-nm filter and imaged with a 512 frame-transfer cooled CCD camera (Princeton Instruments, Inc., Princeton, NJ). Control of image acquisition was achieved using the Metafluor software (Universal Imaging Corp., West Chester, PA), operating on a Pentium Dell computer (Dell Inc., Toronto, Canada). Intracellular calcium was measured using fura-2 AM with the Photon Technologies, Inc. (Santa Clara, CA) system described previously (Kapus et al., 1994).

For imaging experiments, the cells were grown on 25-mm-diam glass coverslips (Thomas Scientific, Swedesboro, NJ) that were inserted into a Leiden CoverSlip Dish (Medical Systems Corp., Greenvale, NY), which was in turn placed into a thermostatted perfusion chamber (Open Perfusion Micro-Incubator; Medical Systems Corp.). Regions of juxtanuclear fluorescence compatible with the morphology and location of the Golgi complex were selected for measurement by the imaging system. Background noncontributory fluorescence emanating mostly from the dark current of the camera was digitally subtracted with each experiment. At the end of each experiment, a calibration curve of fluorescence vs pH was obtained in situ by sequentially perfusing the cells with KCl-rich media (125 mM KCl, 20 mM NaCl, 10 mM Hepes, 10 mM MES, 0.5 mM $CaCl_2$, 0.5 mM $MgCl_2$) containing 5 μM monensin and buffered to pH values ranging from 5.5–7.5. The theoretical basis of this method has been described in detail earlier (Geisow, 1984). Approximately 5 min was allowed for equilibration at each pH.

Results

Subcellular Localization of FITC-VT1B by Confocal Microscopy

The course of FITC-VT1B internalization in Vero cells was monitored by confocal fluorescence microscopy. Representative micrographs are illustrated in Fig. 1. The toxin was initially allowed to bind to surface receptors (Gb_3) at 4°C. At such low temperatures, internalization is precluded and the toxin is restricted to the surface membrane (Fig. 1 *A*). The superficial location was confirmed by cross-sectional reconstruction of serial confocal slices (*z* scan; Fig. 1 *G*). Rapid internalization into a punctate vesicular compartment occurred within 15 min of warming the cells to 37°C (Fig. 1 *B*). By 30 min, punctate staining persisted, but a fraction of the toxin had accumulated in a juxtanuclear region (Fig. 1 *C*). Juxtanuclear fluorescence was predominant after 1 h (Fig. 1 *D*) and remained so for up to 4 h, although some dispersal was evident at 2 and 4 h (Fig. 1, *E* and *F*). Cross-sectional or *z* scans corroborated the deep juxtanuclear position of the toxin after 1 h at 37°C (Fig. 1 *H*).

The identity of the compartment where FITC-VT1B accumulates after internalization was explored by comparison with the location of acknowledged resident proteins of individual organelles. As shown in Fig. 2 *A*, the juxtanuclear structure containing FITC-VT1B (left image in every panel of Fig. 2) is distinct from the more diffuse ER, identified using antibodies to the molecular chaperone calnexin (Jackson et al., 1994). This conclusion was confirmed using Con A, which binds to integral membrane glycoproteins of the ER reticulum and Golgi complex (Tartakoff and Vassalli, 1983). The lectin displayed diffuse staining, with some accumulation in a region near the nucleus that overlapped partially with FITC-VT1B (Fig. 2 *B*). The specificity of the Con A labeling was confirmed by displacement with the competitive ligand, α-methyl-mannoside (not shown).

The compartment containing the internalized toxin was also readily distinguishable from lysosomes. The latter, identified using overnight fluid-phase uptake of FITC-dextran (Geisow, 1984), were homogeneously dispersed throughout the cytosol and were, in fact, preferentially excluded from the regions labeled by FITC-VT1B (Fig. 2 *C*). Transferrin, which reaches sorting and recycling endosomes via clathrin-coated pits (Lamb et al., 1983), was also localized in a compartment clearly different from the structure containing FITC-VT1B (Fig. 2 *D*). Finally, MitoTracker, a novel mitochondrial marker, identified elongated structures that were adjacent yet distinct from those accumulating FITC-VT1B (Fig. 2 *E*). Jointly, these findings rule out the possibility that the ER, early endosomes, lysosomes, and mitochondria are the organelles where most of the FITC-VT1B is located in cells incubated with the toxin for 1–2 h.

The juxtanuclear localization of FITC-VT1B fluorescence is suggestive of Golgi localization. A number of markers of various components of the Golgi complex were tested in dual-labeling experiments (Fig. 3). NBD-ceramide, a fluorescent lipid with high affinity for Golgi membranes (Pagano et al., 1991), showed extensive colocalization with FITC-VT1B in a crescent-shaped perinuclear structure characteristic of the Golgi apparatus (Fig. 3 *A*). Similarly, the staining pattern of WGA, which binds preferentially to membrane glycoproteins of the Golgi stacks (Tartakoff and Vassalli, 1983), was very similar to that of the toxin (Fig. 3 *B*). Specificity of the lectin binding was confirmed using *N*-acetylglucosamine (not shown). The site of toxin accumulation was, in addition, found to overlap precisely with the distribution of the *cis*-Golgi markers, β-COP (Serafini et al., 1991) (Fig. 3 *C*) and the 10E6 antigen (Wood et al., 1991) (see Fig. 5 *B*), and with α-mannosidase II (Fig. 3 *D*), a resident membrane protein of the medial and *trans* cisternae of the Golgi stack (Velasco et al., 1993). These findings strongly suggest that FITC-VT1B is concentrated in the Golgi complex of Vero cells, and similar results were obtained with HeLa cells (not shown). The specific Golgi subcompartment(s) containing the toxin could not be identified, as they cannot be resolved by confocal fluorescence microscopy.

Two additional lines of evidence support the localization of FITC-VT1B in the Golgi apparatus of Vero cells. First, the toxin was found to colocalize with the microtubule organizing center (Fig. 4 *A*). This is the expected location of the Golgi apparatus, which is maintained in its juxtanuclear position by centripetal movement along microtubules (Ayscough et al., 1993). Accordingly, treatment

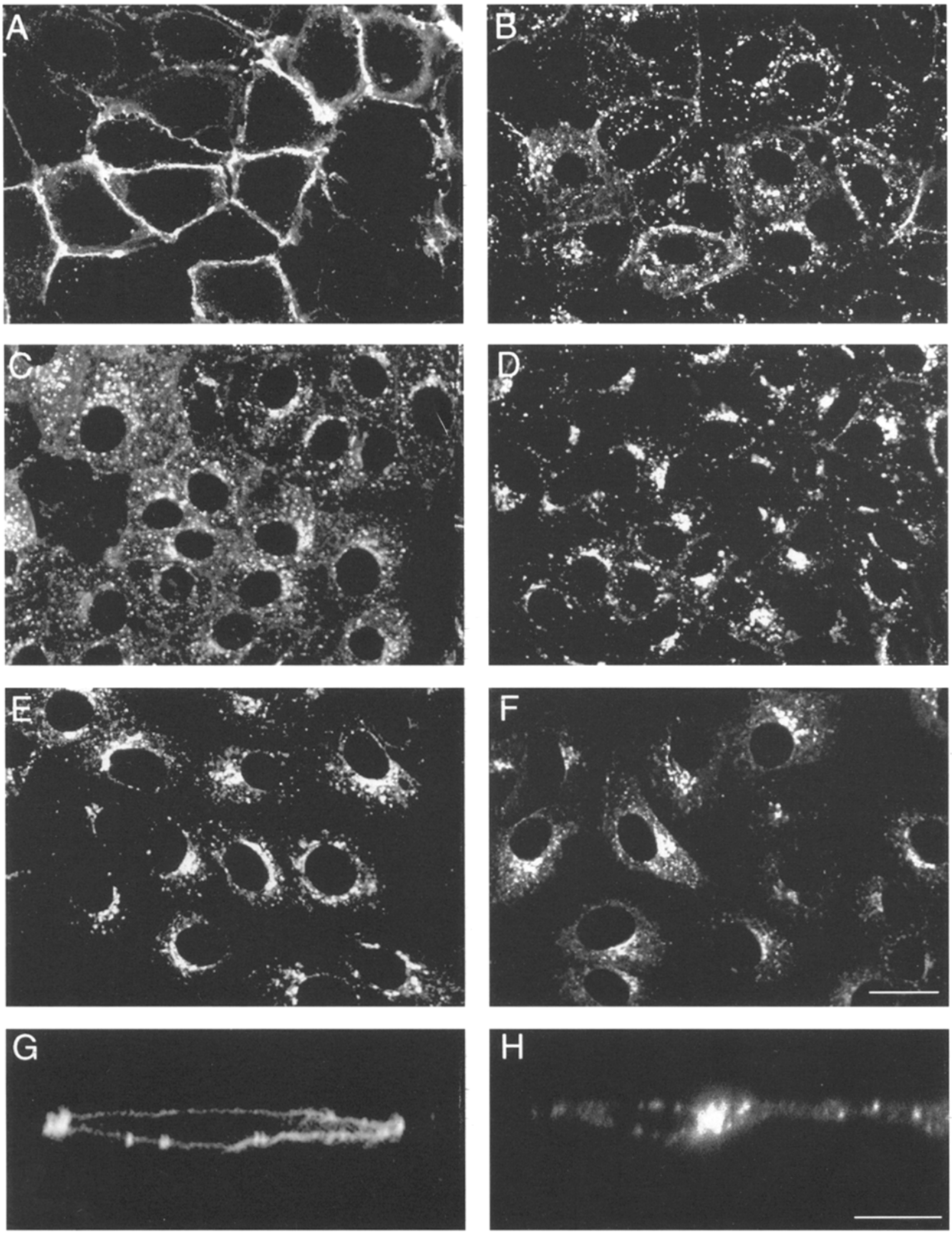

Figure 1. Time course of FITC-VT1B internalization. Vero cells grown on glass coverslips were incubated with 10 μg/ml FITC-VT1B in PBS at 4°C for 1 h. Cells were then incubated for the indicated periods of time at 37°C and fixed with paraformaldehyde. Coverslips were mounted and visualized under confocal microscopy. *x* vs *y* scans (*A–F*) or *x* vs *z* (cross-sectional) reconstructions (*G* and *H*) are shown. *A* = 0 min; *B* = 15 min; *C* = 30 min; *D* = 1 h; *E* = 2 h; *F* = 4 h; *G* = 0 min; *H* = 1 h. Bars, 5 μm.

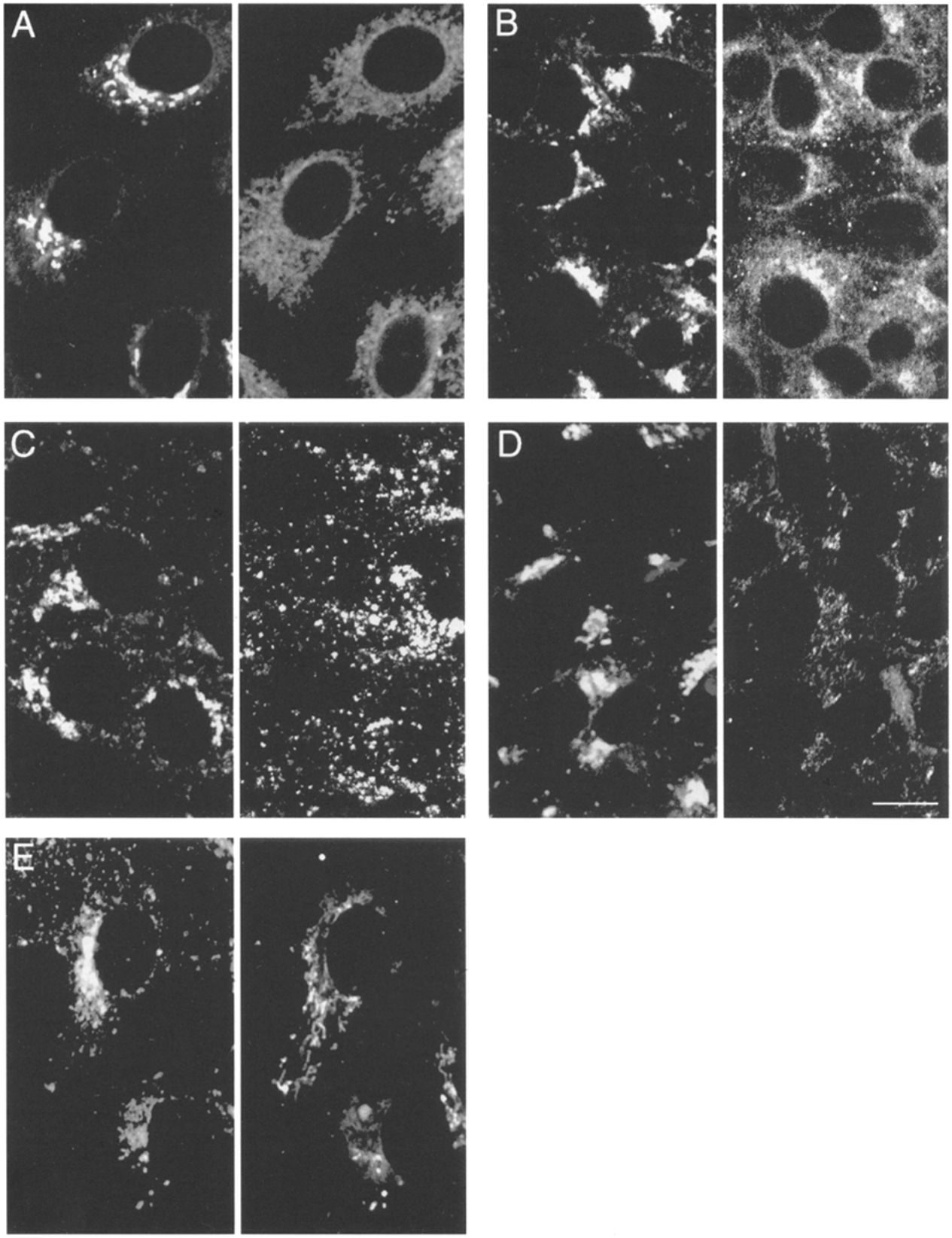

Figure 2. Comparison of the subcellular localization of VT1B with specific organellar markers. Vero cells were incubated with FITC-VT1B or RITC-VT1B in PBS at 4°C for 1 h, and then incubated for 1 h at 37°C, fixed, and permeabilized. The left section of each panel illustrates VT1B staining. The cells were additionally stained with organellar-specific fluorescent markers, and the results are shown in the right section of each panel, as follows: (*A*) calnexin (indirect immunofluorescence); (*B*) Texas red–labeled Con A (2–5 μg/ml); (*C*) lysosomal labeling (overnight incubation with FITC-dextran); (*D*) Texas red–labeled transferrin (2–5 μg/ml, 10-min pulse); (*E*) mitochondrial labeling (MitoTracker®). Bar (applies to all panels), 5 μm.

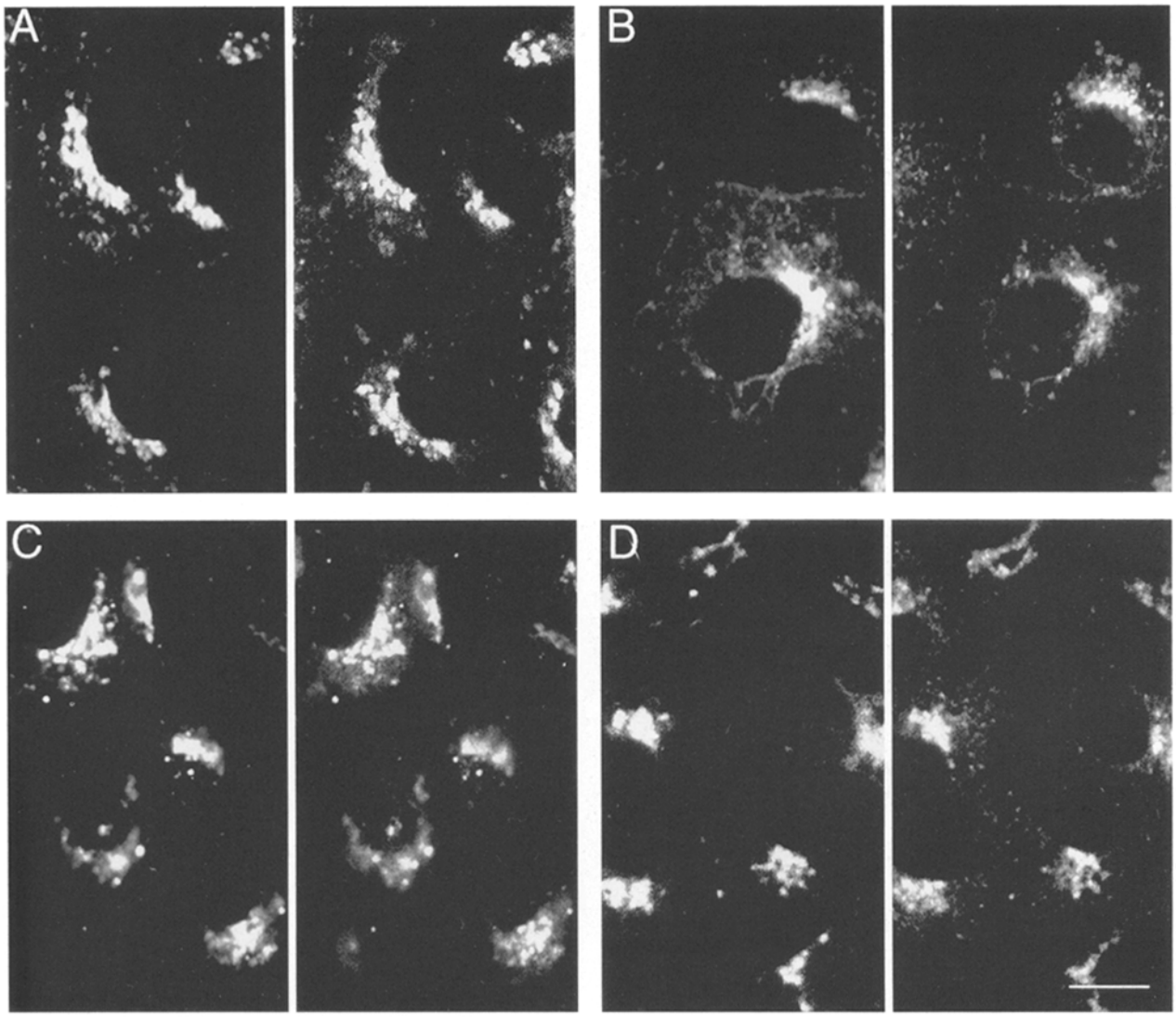

Figure 3. Colocalization of VT1B with Golgi complex markers. Vero cells were labeled with FITC-VT1B or RITC-VT1B as in Fig. 2. The results are shown in the left section of each panel. The cells were additionally stained with several Golgi-specific markers, and the results are shown in the right section of each panel, as follows: (*A*) NBD-ceramide (25 μg/ml at 37°C for 10 min); (*B*) WGA (37°C for 30 min); (*C*) β-COP (indirect immunofluorescence); (*D*) α-mannosidase II (indirect immunofluorescence). Bar, 5 μm.

of the cells with colchicine, which disrupts microtubular structure (Fig. 4 *C*, *right*) and is known to redistribute the Golgi complex (Turner and Tartakoff, 1989), resulted in dispersal of FITC-VT1B throughout the cell (Fig. 4 *C*, *left*). Secondly, the FITC-VT1B–associated fluorescence was also redistributed upon addition of brefeldin A (Fig. 4 *B*), a yeast metabolite known to disrupt the structure of the Golgi complex (Wood et al., 1991; Lippincott-Schwartz et al., 1989; Fujiwara et al., 1988). The sensitivity to colchicine and brefeldin A, together with the precise colocalization with a variety of markers of the Golgi apparatus, indicates that FITC-VT1B accumulates preferentially in this organelle and can, in principle, be used to deliver pH-sensitive probes.

Effect of VT1B on Cell Viability and Golgi Function

In susceptible cells, the VT1 holotoxin induces cell death by inhibition of protein synthesis (Obrig et al., 1985). Although the isolated B subunit lacks RNase activity, it nevertheless has been reported to induce apoptosis in some cell types (Mangeney et al., 1993). It was therefore important to establish whether FITC-VT1B had deleterious effects in our experiments. Viability, assessed by exclusion of Trypan blue, remained unaltered in cells treated with the toxin for up to 24 h (not shown). The ability of the cells to replicate, determined by counting the cells with a Coulter counter, was somewhat reduced (~25%) after 24 h.

The morphology of the Golgi complex was unaffected by introduction of the toxin. When the appearance of the Golgi was compared in cells treated with or without VT1B using the *cis*-Golgi marker 10E6 (Wood et al., 1991), the results were indistinguishable (Fig. 5, *A* and *B*, *left*). The precise colocalization of 10E6 and FITC-VT1B (Fig. 5, *B*, compare *right* and *left*) confirms that the toxin accumulates in the Golgi complex. Moreover, the distribution of the medial- and *trans*-Golgi marker α-mannosidase II was also similar whether the cells were treated with toxin or not (Fig. 5, *C* and *D*). Thus, FITC-VT1B appears to be in-

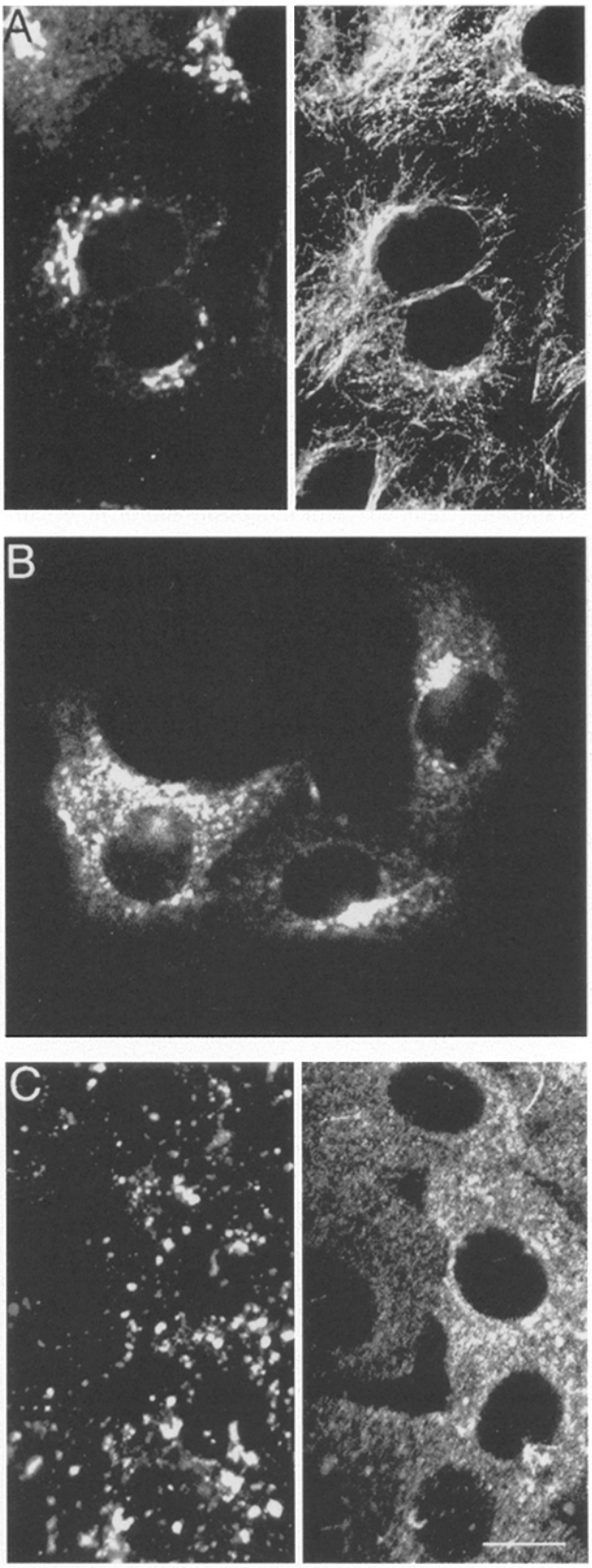

Figure 4. Effects of brefeldin A and colchicine on FITC-VT1B localization. Cells were stained with FITC-VT1B as in Fig. 2. In addition, microtubules were stained by indirect immunofluorescence with anti-tubulin antibody (*A* and *C*, *right*). (*A*) Stained but otherwise untreated cells. (*Left*) FITC-VT1B; (*right*) tubulin. (*B*) FITC-VT1B distribution in cells treated with brefeldin A (5 μg/ml). (*C*) Cells treated with colchicine (0.5 mM). (*Left*) FITC-VT1B; (*right*) tubulin. Bar, 5 μm.

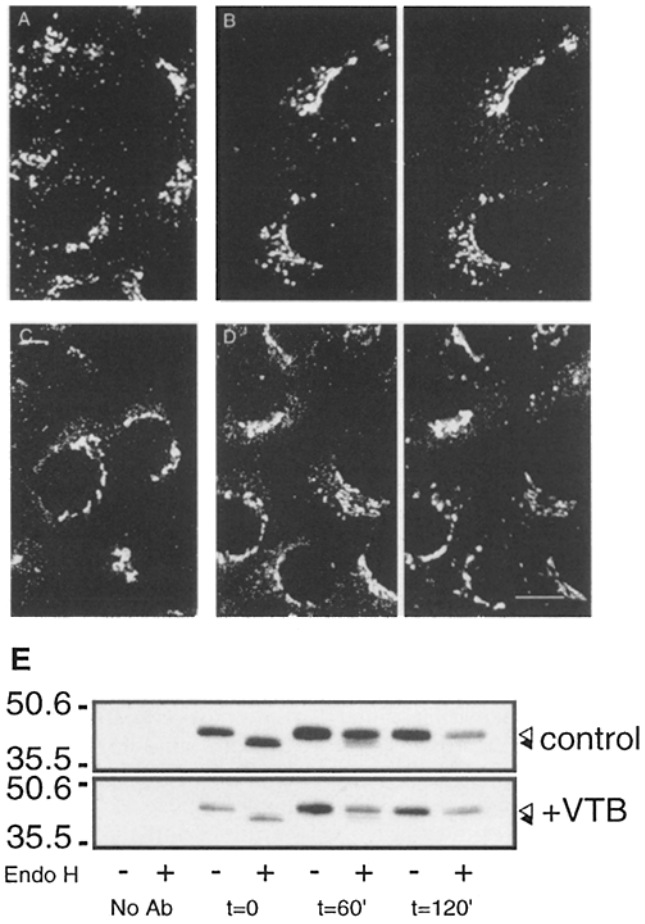

Figure 5. VT1B does not alter Golgi structure or function. (*A*) Staining of the *cis*-Golgi cisternae of otherwise untreated cells by indirect immunofluorescence with the monoclonal 10E6 antibody. (*B*) Cells were treated with FITC-VT1B as in Fig. 2, and then fixed and labeled with 10E6 as in *A*. (*C*) Staining of the medial and *trans*-Golgi cisternae of untreated cells by indirect immunofluorescence with antibody to α-mannosidase II. (*D*) Cells were treated with FITC-VT1B as in Fig. 2, and then fixed and labeled with α-mannosidase II antibody as in *C*. In *B* and *D*, the fluorescence of FITC-VT1B is shown in the left panel, while the Golgi markers are shown to the right. (*E*) Effect of VT1B on glycosylation of MHC class I molecules in the Golgi. Cells were treated with or without 10 μg/ml VT1B, allowed to internalize the toxin for 1 h, and then pulsed with [^{35}S]Cys/Met for 15 min. After the indicated chase periods, the cells were lysed, and MHC class I was immunoprecipitated. The precipitates were then treated with (+) or without (−) endoglycosidase H (*Endo H*) and finally analyzed by SDS-PAGE and autoradiography. The glycosylated MHC species are indicated by an open arrow, while the deglycosylated product of Endo H treatment is marked by a solid arrow. The two leftmost lanes are controls without primary antibody. Bar, 5 μm.

nocuous, inasmuch as it does not alter the structure of the Golgi apparatus.

More importantly, Golgi function appeared to proceed normally over extended periods. Two different assays of Golgi function were used. Lipid metabolism was estimated by the method of Ktistakis et al. (1995) using C_5-DMB-ceramide. The fluorescence changes over a 24-h period, indicative of lipid export from the Golgi, were indistinguish-

able between control and VT1B-treated cells (not shown). We also assessed the effect of VT1B on exocytic protein traffic through the Golgi. To this end, we used pulse-chase experiments to determine the rate at which MHC class I molecules acquire Endo H resistance, a consequence of N-linked oligosaccharide processing by enzymes that reside in the Golgi. As shown in Fig. 5 *E*, when treated with endo H immediately after pulsing ($t = 0$), the class I heavy chain undergoes a shift to a lower molecular weight form as a result of the removal of its immature, high mannose–type oligosaccharide. After a 60-min chase, however, most of the protein has become endo H resistant, indicative of oligosaccharide processing by Golgi enzymes. After 120 min, virtually all of the labeled heavy chain has become resistant to endo H. Importantly, the time course and extent to which MHC class I molecules acquired endo H resistance were not altered by prior internalization of VT1B (Fig. 5 *E*, *lower panel*). These findings indicate that the toxin does not alter protein passage through the Golgi stacks and glycosylation therein.

Measurement of Golgi pH

The above results imply that VT1B accumulates in the Golgi complex with minimal disruption of cellular viability or function. The toxin therefore appears suitable to target fluorescent pH-sensitive probes to this organelle. The VT1B monomer, a 7.5-kD polypeptide, possesses one or more lysine residues in its NH_2-terminal domain that can be covalently derivatized without impairment of its Gb_3-binding capacity (Khine et al., 1994). The location of four candidate sites is illustrated in Fig. 6 *A*. To generate probes of Golgi pH, purified recombinant VT1B was covalently linked to fluorescein, a bright, pH-sensitive fluorophore. The spectral properties and pH dependence of the fluorescein derivative were tested and are illustrated in Fig. 6, *B* and *C*. Fluoresceinated VT1B had excitation and emission maxima of 493 and 515 nm, respectively. As with other FITC derivatives, fluorescence decreased with pH, with marginal spectral shifts (Fig. 6, *B* and *C*). Additionally, FITC labeling had no effect on VT1B/Gb3 binding.

FITC-VT1B was internalized by Vero cells, and its fluorescence was readily detectable in viable cells using a sensitive cooled CCD camera. The juxtanuclear position of the fluorescence could be defined by simultaneous observation of the cell morphology by differential interference contrast microscopy (Fig. 7, *A* and *B*). FTIC-VT1B was not noticeably degraded within the Golgi. This was established by electrophoretic analysis of toxin extracted from cells 1 h after internalization (data not shown).

Although the intensity of the excitation beam was minimized, the occurrence of dye photobleaching upon repeated illumination was evident. The fluorescence loss was not due to pH changes, as it persisted in cells where $[H^+]$ was stabilized (clamped) with monensin and/or nigericin. Two independent approaches were used to correct for photobleaching. The first one estimated the fractional loss of dye occurring during each exposure to the excitation beam and compensated for this decrease. Representative experiments are illustrated in Fig. 8 *A*. Under the conditions used, the fraction of fluorescence lost after individual exposures was rather consistent among different cells. A semi-ln plot of the relative fluorescent intensity was adequately fit by linear regression with $r = 0.998$, consistent with first-order kinetics (Fig. 8 *A*, *inset*). The data were described by the equation, $y = y_o + A_1 e^{(x_o - x)/t_1}$, where y_o is the y intercept, and A_1 and t_1 are constants. Using this relationship, the extent of fluorescence loss by photobleaching after a given number of exposures could be predicted and corrected, normalizing the fluorescence to the initial level. The second approach is based on the unequal magnitude of the fluorescence changes at different wavelengths that

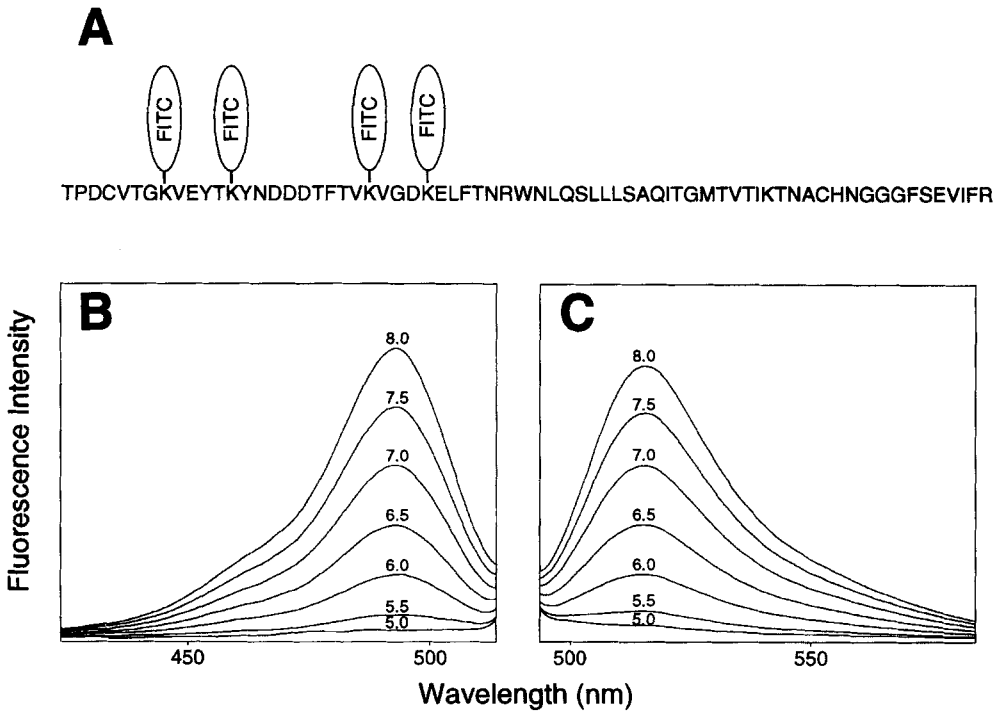

Figure 6. Spectral properties and pH dependence of fluorescent VT1B conjugates. (*A*) Amino acid sequence of the VT1B monomer, indicating the potential sites of FITC binding (see Khine and Lingwood, 1994, for details); excitation (*B*) and emission (*C*) spectra of FITC-VT1B obtained in solutions of the pH indicated on the curves.

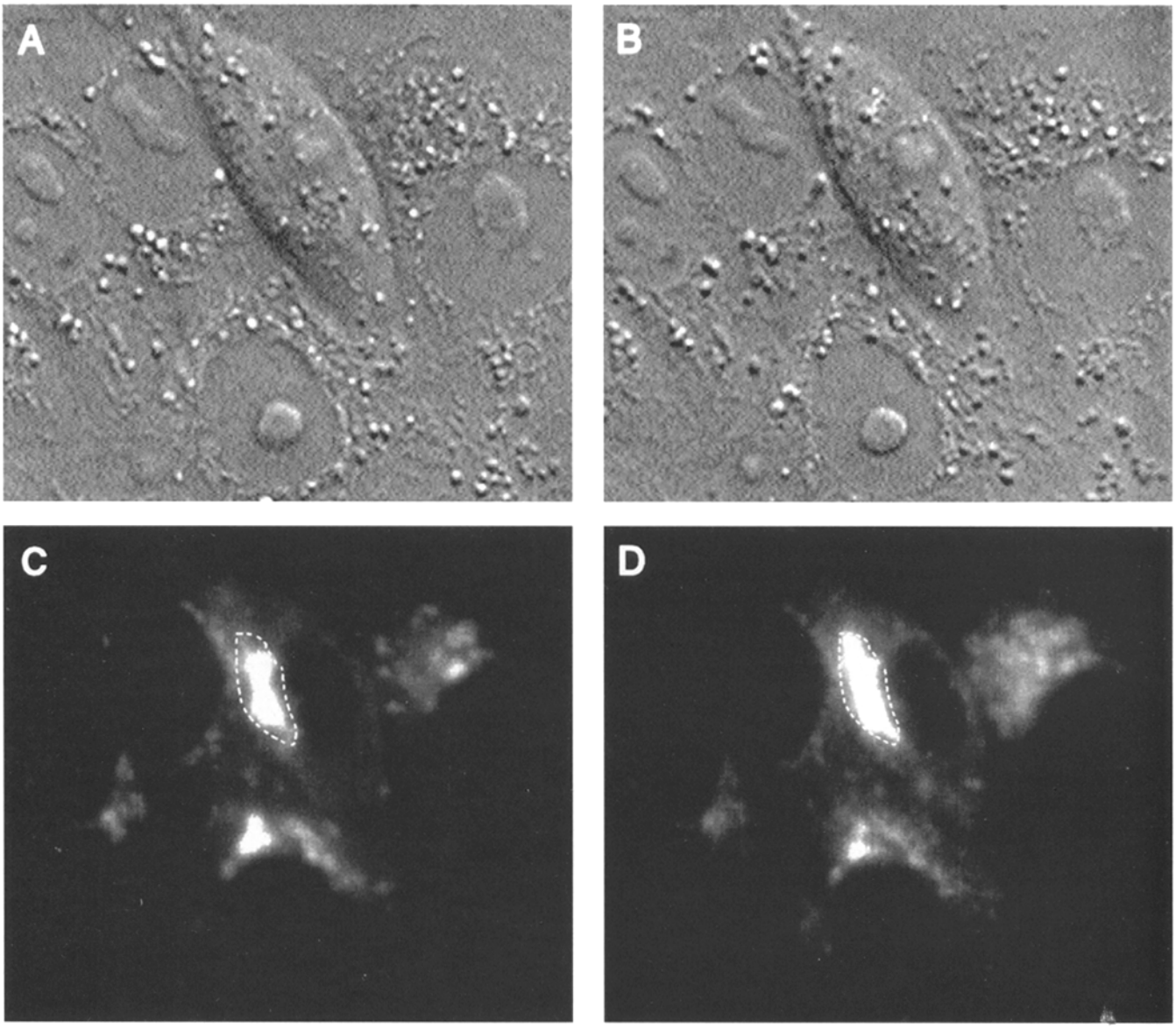

Figure 7. Visualization of VT1B-associated fluorescence in live cells. Vero cells were incubated with FITC-VT1B for 1 h at 4°C, followed by a 1-h chase at 37°C. (*A* and *B*) Nomarski images of cells before and 15 min after treatment with monensin (5 μg/ml). (*C* and *D*) Corresponding fluorescence images, acquired with a cooled CCD camera. (*Dashed line*) Region of interest chosen for measurement of fluorescence intensity.

occur when the pH of the medium is varied. The ratio of the fluorescence intensity with excitation at 490/440 nm remains constant despite photolysis of the dye. Both procedures were used and yielded almost identical results.

The fluoresceinated derivative of VT1B retains sensitivity to pH after being internalized to the Golgi. This was demonstrated by equalizing the luminal pH of the Golgi with that of the cytosol, which is in turn made equal to that of the external medium, using the alkali cation/H^+ exchanger monensin. Equalization of pH in all compartments is predicated on the assumption that the total monovalent cation concentration of all compartments is comparable. This assumption is reasonable, since all the compartments are at osmotic equilibrium and K^+ and Na^+ are the main cationic osmolytes of mammalian cells. A typical calibration of FITC-VT1B fluorescence at 490 nm vs pH in situ is shown in Fig. 8 *B*, while a plot of the 490/440 nm ratio vs pH is illustrated in Fig. 8 *C*. The pH dependence of the toxin in the Golgi is indistinguishable from that measured in solution (Fig. 8 *B*, *solid triangles*), with half-maximal fluorescence near pH 6.5. This property renders the probe most sensitive near the pH anticipated for intracellular organelles.

Prolonged exposure to monensin has been shown to cause swelling of the Golgi complex and perturbation of secretory function in certain cells (Tartakoff, 1983*b*). At the concentration used (5 μg/ml), monensin equilibrates protons across both plasma and Golgi membranes within 5 min. In Vero cells, small but visible changes to Golgi morphology occurred during the course of the calibration procedure (see Fig. 7, *C* and *D*). When defining the region of interest for analysis of fluorescence, care was taken to ac-

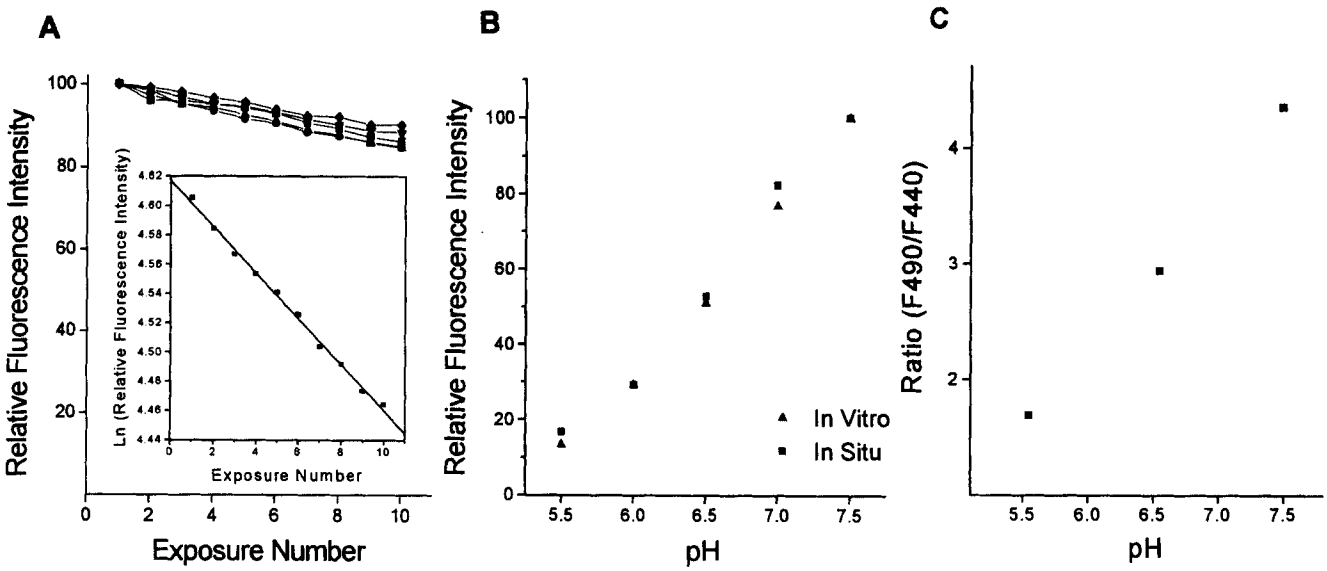

Figure 8. Photobleaching and calibration of internalized FITC-VT1B. (*A*) Loss of FITC-VT1B fluorescence intensity upon repeated exposure to 500-ms excitation pulses. Data from five independent cells are illustrated in the main panel. (*Inset*) Semi-logarithmic curve of the average fluorescence vs the exposure number. The line was fitted assuming first-order kinetics ($r = 0.998$). (*B*) The fluorescence intensity of FITC-VT1B (490 nm excitation) was measured as a function of pH both in solution (*In Vitro*) as described in Fig. 6 (*triangles*), and within the Golgi of Vero cells (*In Situ*; *squares*). The data was normalized to the fluorescence at pH 7.5 to allow comparison. (*C*) Relationship between pH and fluorescence ratio (490/440 nm), measured in situ. The pH of the Golgi within intact cells was manipulated with ionophores, as described in Materials and Methods. Data are representative of 90 experiments.

count for any displacement of fluorescent toxin, and a threshold was applied to intensity values to eliminate the contribution of adjacent background fluorescence (e.g., Fig. 7).

The pH of the Golgi (pH_G) of intact Vero cells was measured using the photobleaching correction and calibration procedures described above. Using the single wavelength method, pH_G measured at 37°C averaged 6.42 ± 0.05 (mean ± SEM), while at room temperature (~20°C), pH_G was somewhat lower, averaging 6.36 ± 0.05 ($n = 11$; Table I). Ratiometric fluorescence measurements (Fig. 9) yielded an average pH_G of 6.45 ± 0.03 at 37°C ($n = 90$). Although the absolute pH values estimated by the two procedures were not identical, the relative changes noted with inhibitors and weak electrolytes were very similar. Therefore, the two methods were used indistinctly hereafter.

Mechanism of pH_G Regulation

In otherwise untreated cells, pH_G remained constant over extended periods of analysis (up to 20 min). Moreover, acute changes in extracellular pH over a range of 5.5 and 7.5 did not result in measurable alterations of pH_G (Table I), attesting to the preserved integrity of the cell and Golgi complex and suggesting the presence of an active, continuously regulated process. In organelles of the endocytic pathway, as well as in secretory granules, luminal acidification is mediated by a V-type ATPase (Forgac, 1992). This type of ATPase is selectively inhibited by macrolide antibiotics such as the bafilomycins and concanamycins. As shown in Fig. 10 *A*, addition of 500 nM bafilomycin A to Vero cells induced a rapid increase in pH_G, implying that a V-ATPase is essential for maintenance of the luminal acidification. The rapid dissipation of the transmembrane pH gradient indicates that the Golgi membrane is substantially permeable to H^+ (equivalents). Alternatively, rapid import of fluid with higher pH by vesicular transport could account for the observed alkalinization.

To evaluate whether the $[H^+]$ of the Golgi is regulated, pH_G was displaced from its steady state using NH_4Cl (Fig. 10 *B*). A rapid alkalinization, presumably resulting from entry of ammonia, was recorded. This was immediately followed by a reacidification toward the original pH_G. The latter may reflect entry of ammonium or activation of an active acidifying process. The latter interpretation is supported by two findings: (*a*) a comparable reacidification was also observed when the cells were challenged with trimethylammonium, a much larger and less permeable cation (Fig. 10 *B*, *inset*); and (*b*) addition of bafilomycin inhibited the pH recovery after addition of ammonium (not shown). These findings favor the notion that the observed secondary acidification was due to active pH_G regulation by the proton pump rather than to permeation of the protonated base. In cells that had recovered after addition of

Table I. Effect of Temperature and Extracellular pH on Golgi pH

	Condition	Measured pH (± SEM)
Changes in temperature	RT	6.36 ± 0.05
	37°C	6.42 ± 0.05
Changes in extracellular pH	pH 5.5	6.39 ± 0.14
	pH 6.5	6.37 ± 0.13
	pH 7.5	6.41 ± 0.16

Vero cells were loaded with FITC-VT1B, and fluorescence was measured as described in Materials and Methods. Cells were then incubated at room temperature (RT ~ 20°C) or 37°C for 10 min before measurement of pH_G. For external pH changes, the cells were incubated in calibration solutions identical to those used in Fig. 9, but without monensin.

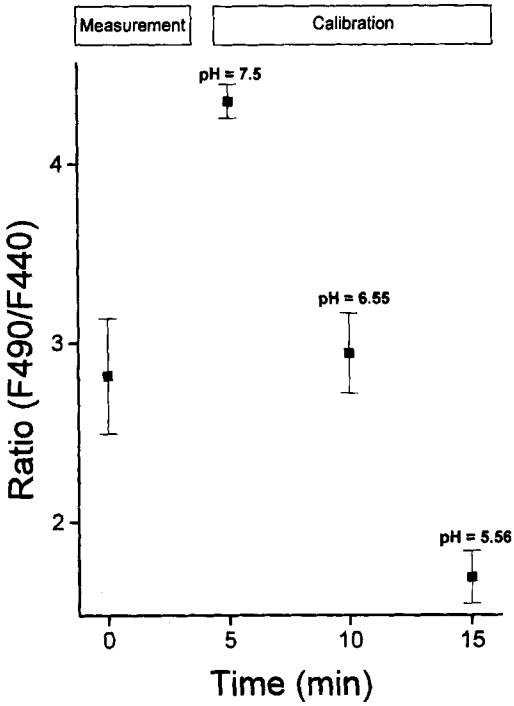

Figure 9. Measurement of Golgi pH. Vero cells were loaded with FITC-VT1B, and fluorescence was measured with the cooled CCD camera as described in Materials and Methods. The 490/440-nm fluorescence ratio was recorded from untreated cells at 37°C (measurement). Cells were then bathed in calibration solutions (125 mM KCl, 20 mM NaCl, 10 mM Hepes, 10 mM MES, 0.5 mM $CaCl_2$, 0.5 mM $MgCl_2$) containing monensin (5 μM), and pH varied between 7.5 and 5.5. Data are means ± SEM of the ratios of 90 individual experiments.

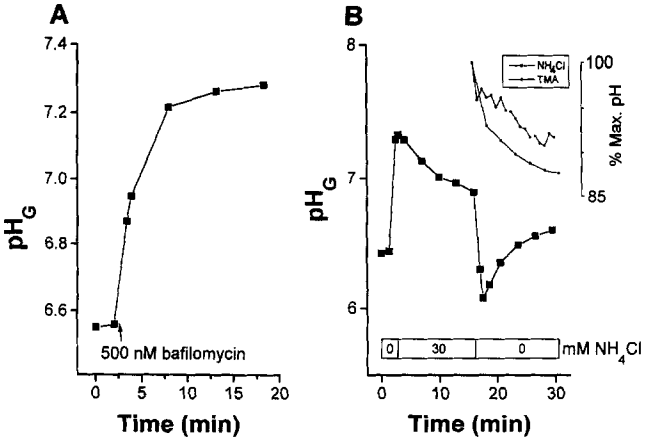

Figure 10. Effects of bafilomycin and ammonium on Golgi pH. The Golgi pH (pH_G) of Vero cells was measured as in Fig. 9. (*A*) pH_G measurements before and after addition of 500 nM bafilomycin A_1. (*B*) Where indicated, the cells were exposed to 30 mM NH_4Cl, followed by its removal. Data are representative of six similar experiments. (*Inset*) Comparison of the pH_G transients induced by 30 mM NH_4Cl (*squares*) and trimethylamine (*TMA*; *circles*). Data were normalized to facilitate the comparison.

NH_4^+, removal of the cation produced a sudden acidification, as a result of loss of ammonia, that undershot the initial pH_G. Subsequently, pH_G increased back to or near the original level, consistent with the existence of a regulatory process.

Unlike the effect of weak bases, no significant pH_G changes were recorded upon introduction of CO_2, which is in equilibrium with the weak acid H_2CO_3 (not shown). The permeability of the weak acid is difficult to assess from these experiments, since its pK_a is of the same order as pH_G. It can, however, be speculated that the conjugate base bicarbonate, which is not at chemical equilibrium, has limited permeability. Confirmation of this hypothesis requires determination of the electrical potential across the Golgi membrane.

We next studied the dependence of pH_G on the cytosolic pH. This analysis required us to manipulate the cytosolic pH by means that would not directly alter pH_G. This was accomplished by operating the plasmalemmal Na^+/H^+ exchanger in reverse. To this end, cells were initially loaded with Na^+ by incubation in K^+-free medium with ouabain for 1 h. Extracellular Na^+ was then suddenly replaced by the impermeant cation *N*-methyl-D-glucammonium$^+$. The imposed outward Na^+ gradient can drive the exchanger in reverse, promoting a gradual cytosolic acidification. The validity of this approach was confirmed in cells loaded with 2′, 7′-bis(carboxyethyl)-carboxylfluorescein (BCECF) to monitor the cytosolic pH (Paradiso et al., 1984). As shown in Fig. 11 *A*, the cytosol underwent a ~0.6 pH unit acidification within 15–20 min. pH_G was next measured in parallel cells subjected to an identical protocol. As illustrated in Fig. 11 *B*, pH_G remained essentially constant throughout the period of cytosolic acidification. These observations suggest that pH_G is regulated independently of the surrounding cytosolic pH.

Finally, we tested whether pH_G was affected by changes in cytosolic $[Ca^{2+}]$ within the physiological range. Thapsigargin triggers an increase in cytosolic $[Ca^{2+}]$ as a result of spontaneous leakage of the cation from the ER, followed by opening of plasmalemmal channels (Thastrup et al., 1990). Treatment with thapsigargin, an inhibitor of endomembrane Ca^{2+} pumps, had no discernible effect on pH_G in either Vero or HeLa cells (Fig. 12 *B*). The occurrence of a $[Ca^{2+}]$ elevation under the conditions of our experiments was confirmed in HeLa cells using fura-2 (Fig. 12 *A*), but could not be directly documented in Vero cells, which were found not to retain any of the Ca^{2+}-sensitive probes tested, including fura-2, indo-1, and fluo-3.

Discussion

In principle, the internal pH of individual organelles can be studied after fractionation, using either spectroscopic or isotopic methods (Glickman et al., 1983). It is clear, however, that organelles undergo varying degrees of damage during the homogenization and subcellular fractionation procedures. Moreover, the influence of soluble or loosely associated regulatory factors would be lost under such conditions. For these reasons, in situ analysis of organellar pH is preferable. Two methods had been reported earlier for direct assessment of the pH of components of the secretory pathway within intact cells. The first utilizes DAMP, a permeant weak base that partitions preferentially in acidic organelles, where it can be fixed and detected by immunogold. Using this approach, the *trans-*

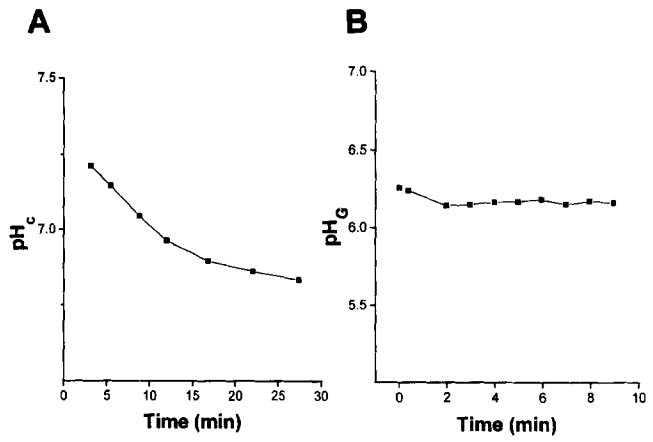

Figure 11. Effect of changing cytosolic pH on Golgi pH. Vero cells were loaded with Na^+ by incubation in PBS containing 1 mM $CaCl_2$, 1 mM $MgCl_2$, pH 7.4, with 1 mM ouabain at 37°C for 45 min. Cells were then perfused with an *N*-methyl-D-glucammonium$^+$-based, Na^+-free medium to induce reversal of Na^+/H^+ exchange. (*A*) Measurement of cytosolic pH (pH_c) using BCECF; (*B*) parallel measurements of Golgi pH (pH_G). Representative of six experiments.

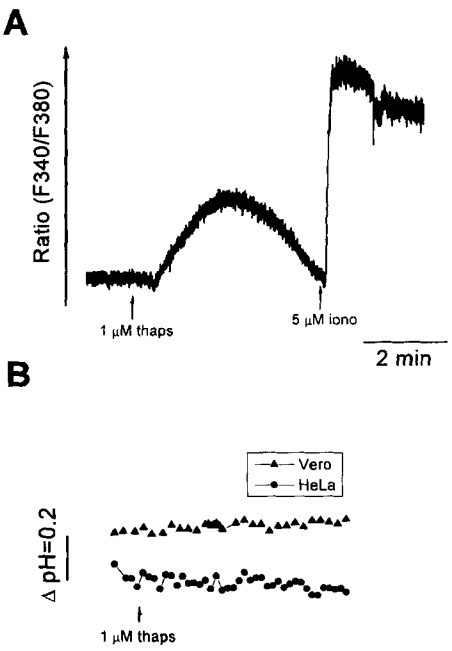

Figure 12. Effect of changing cytosolic Ca^{2+} on Golgi pH. (*A*) HeLa cells were loaded with Fura-2, and the fluorescence ratio (F340/F380), an estimate of $[Ca^{2+}]$, was measured. Where noted, the cells were treated with 1 μM thapsigargin (*thaps*), followed by 5 μM ionomycin (*iono*); (*B*) pH_G was measured in Vero and HeLa cells, as in Fig. 9. Where noted, the cells were treated with 1 μM thapsigargin to transiently increase $[Ca^{2+}]$.

Golgi was found to be acidic with respect to the cytosol (Anderson and Pathak, 1985). However, acidotropic electron-dense markers are not ideal for the systematic study of Golgi pH regulation for several reasons. Owing to the need for sample fixation, the procedure is static, precluding continuous recording of pH under varying conditions. Secondly, sample processing is time consuming and comparatively expensive. Finally, the quantitative resolution of the method is limited.

While this work was in progress, a second method was described for measurement of *trans*-Golgi pH, based on the delivery of fluorescent indicators by microinjection of liposomes (Seksek et al., 1995). This approach overcomes some of the limitations of DAMP, allowing continuous recording at considerably lower cost. The requirement for liposome microinjection, however, implies that the procedure is very laborious and invasive. Insertion of liposomal lipids into the membranes of the Golgi, and dilution of the contents of the latter with the liposomal contents, is bound to alter the function and buffering power of the organelle. Finally, with this procedure, measurements under physiological conditions are restricted to a window of a few minutes, since the fluid-phase indicator dye is rapidly transported out of the Golgi at 37°C (Seksek et al., 1995).

Most of the shortcomings of the two preceding methods are overcome by the procedure described in this report. The measurements are comparatively simple and inexpensive, allowing continued monitoring at physiological temperature for hours. Based on the criteria tested, treatment of the cells with VT1B is virtually noninvasive, preserving cell viability as well as Golgi morphology and function. While the effect of the FITC-VT1B itself on pH_G cannot be assessed independently, it is noteworthy that this subunit of the toxin binds to the head group of Gb_3, and is not a priori expected to have transmembrane effects, since the toxic A subunit is absent.

The precise location of the fluorescent VT1B within the Golgi complex was not defined in our experiments. However, the collapse of some of the labeled structures onto perinuclear cisternae after treatment with brefeldin A suggests that FITC-VT1B reached the Golgi stack, which under these conditions is known to fuse retrogradely with the ER (Wood et al., 1991). This conclusion is consistent with observations made using Shiga toxin, which is virtually identical to VT1. In HeLa cells studied by EM, Shiga toxin was found in both lateral (*cis* or *trans*) as well as medial cisternae of the Golgi stack (Sandvig et al., 1992).

In 90 experiments using the ratio method, pH_G in Vero cells at 37°C averaged 6.45, over 0.6 U more acidic than the cytosol (determined to have a pH of ~7.1 using BCECF). This transmembrane pH gradient was rapidly dissipated by bafilomycin A_1, implying mediation by a V-type H^+ pump. These findings resemble those of Seksek et al. (1995) and are in accordance with fractionation studies that reported V-ATPase activity in purified Golgi preparations (Glickman et al., 1983). V-type ATPases have also been implicated in the acidification of endosomes and lysosomes, which can have a substantially lower pH. The determinants of the specific pH of individual organelles remain obscure. Distinct isoforms of one or more subunits of the ATPase could, in principle, be responsible for the differential pH. Variations in counterion permeability, suggested to modulate V-ATPase activity (Barasch et al., 1991), could account for differences in the rate of acidification, but not in the steady state pH. An alternative hypothesis postulates that the rates of H^+ pumping are dictated by the abundance of pumps, which vary in different organelles. Alternatively, constant rates of pumping

could be differentially offset by varying H^+ "leakage," resulting in higher pH in organelles with greater passive leak. The two latter hypotheses, however, imply that the steady state pH is a fortuitous combination of unregulated pumps and leaks. Two observations argue against this simplistic notion. First, pH_G remained remarkably constant despite sizable changes in cytosolic pH, which should have affected the pump and leak in opposite directions. Secondly, addition of ammonia, which effectively increases the leak of H^+ equivalents, resulted in a transient alkalosis, but pH_G tended to recover toward its original level shortly thereafter. These findings suggest that pH_G is tightly regulated and that the rate of pumping may adjust to the magnitude of the leak. It is conceivable that ancillary regulators, unique to individual organelles, may dictate the activation threshold and rate of the ATPases, and hence the characteristic pH of each organelle.

In summary, we have been able to harness the unique retrograde pathway used by VT1 to reach the Golgi complex of intact viable cells. By covalently incorporating an $[H^+]$-sensitive moiety to the B subunit of VT1, we were able to determine the pH of the lumen of the Golgi apparatus in a noninvasive manner. The data obtained using this procedure indicate that the Golgi is maintained at an acidic level by means of V-ATPases, despite the presence of a large H^+ (equivalent) leak pathway. The pH of the Golgi is controlled independently of the cytosolic and extracellular pH as well as cytosolic calcium. This approach can be used to follow pH_G in cells under various experimental conditions and to assess the validity of the hypothesis that CFTR, the cystic fibrosis gene product, modulates Golgi function by dictating its pH (Barasch et al., 1991). Moreover, a similar method can be used to deliver probes sensitive to calcium and other biologically relevant substrates to the Golgi. These experiments are currently underway.

J.H. Kim was supported by the Canadian Cystic Fibrosis Foundation (CCFF) and Janssen Ortho Incorporated. This study was supported by the CCFF and the Medical Research Council of Canada. S. Grinstein is an International Scholar of the Howard Hughes Medical Institute.

Received for publication 10 January 1996 and in revised form 10 June 1996.

References

Anderson, R.G., and R.K. Pathak. 1985. Vesicles and cisternae in the trans Golgi apparatus of human fibroblasts are acidic compartments. *Cell.* 40:635–643.

Anderson, R.G., J.R. Falck, J.L. Goldstein, and M.S. Brown. 1984. Visualization of acidic organelles in intact cells by electron microscopy. *Proc. Natl. Acad. Sci. USA.* 81:4838–4842.

Ayscough, K., N.M. Hajibagheri, R. Watson, and G. Warren. 1993. Stacking of Golgi cisternae in *Schizosaccharomyces pombe* requires intact microtubules. *J. Cell Sci.* 106:1227–1237.

Barasch, J., B. Kiss, A. Prince, L. Saiman, D. Gruenert, and Q. al-Awqati. 1991. Defective acidification of intracellular organelles in cystic fibrosis [see comments]. *Nature (Lond.).* 352:70–73.

Boulanger, J., M. Huesca, S. Arab, and C.A. Lingwood. 1994. Universal method for the facile production of glycolipid/lipid matrices for the affinity purification of binding ligands. *Anal. Biochem.* 217:1–6.

Forgac, M. 1992. Structure and properties of the coated vesicle (H+)-ATPase. *J. Bioenerg. Biomembr.* 24:341–350.

Fujiwara, T., K. Oda, S. Yokota, A. Takatsuki, and Y. Ikehara. 1988. Brefeldin A causes disassembly of the Golgi complex and accumulation of secretory proteins in the endoplasmic reticulum. *J. Biol. Chem.* 263:18545–18552.

Galloway, C.J., G.E. Dean, M. Marsh, G. Rudnick, and I. Mellman. 1983. Acidification of macrophage and fibroblast endocytic vesicles in vitro. *Proc. Natl. Acad. Sci. USA.* 80:3334–3338.

Geisow, M.J. 1984. Fluorescein conjugates as indicators of subcellular pH. A critical evaluation. *Exp. Cell Res.* 150:29–35.

Glickman, J., K. Croen, S. Kelly, and Q. Al-Awqati. 1983. Golgi membranes contain an electrogenic H+ pump in parallel to a chloride conductance. *J. Cell Biol.* 97:1303–1308.

Jackson, M.R., M.F. Cohen-Doyle, P.A. Peterson, and D.B. Williams. 1994. Regulation of MHC class I transport by the molecular chaperone, calnexin (p88, IP90). *Science (Wash. DC).* 263:384–387.

Kapus, A., S. Grinstein, S. Wasan, R. Kandasamy, and J. Orlowski. 1994. Functional characterization of three isoforms of the Na+/H+ exchanger stably expressed in Chinese hamster ovary cells. ATP dependence, osmotic sensitivity, and role in cell proliferation. *J. Biol. Chem.* 269:23544–23552.

Khine, A.A., and C.A. Lingwood. 1994. Capping and receptor-mediated endocytosis of cell-bound verotoxin (Shiga-like toxin). 1: Chemical identification of an amino acid in the B subunit necessary for efficient receptor glycolipid binding and cellular internalization. *J. Cell. Physiol.* 161:319–332.

Ktistakis, N.T., C.Y. Kao, R.H. Wang, and M.G. Roth. 1995. A fluorescent lipid analogue can be used to monitor secretory activity and for isolation of mammalian secretion mutants. *Mol. Biol. Cell.* 6:135–150.

Lamb, J.E., F. Ray, J.H. Ward, J.P. Kushner, and J. Kaplan. 1983. Internalization and subcellular localization of transferrin and transferrin receptors in HeLa cells. *J. Biol. Chem.* 258:8751–8758.

Lippincott-Schwartz, J., L.C. Yuan, J.S. Bonifacino, and R.D. Klausner. 1989. Rapid redistribution of Golgi proteins into the ER in cells treated with brefeldin A: evidence for membrane cycling from Golgi to ER. *Cell.* 56:801–813.

Mangeney, M., C.A. Lingwood, S. Taga, B. Caillou, T. Tursz, and J. Wiels. 1993. Apoptosis induced in Burkitt's lymphoma cells via Gb3/CD77, a glycolipid antigen. *Cancer Res.* 53:5314–5319.

Mellman, I., and K. Simons. 1992. The Golgi complex: in vitro veritas? *Cell.* 68: 829–840.

Mellman, I., R. Fuchs, and A. Helenius. 1986. Acidification of the endocytic and exocytic pathways. *Annu. Rev. Biochem.* 55:663–700.

Obrig, T.G., T.P. Moran, and R.J. Colinas. 1985. Ribonuclease activity associated with the 60S ribosome-inactivating proteins ricin A, phytolaccin and Shiga toxin. *Biochem. Biophys. Res. Commun.* 130:879–884.

Ohkuma, S., and B. Poole. 1978. Fluorescence probe measurement of the intralysosomal pH in living cells and the perturbation of pH by various agents. *Proc. Natl. Acad. Sci. USA.* 75:3327–3331.

Pagano, R.E., O.C. Martin, H.C. Kang, and R.P. Haugland. 1991. A novel fluorescent ceramide analogue for studying membrane traffic in animal cells: accumulation at the Golgi apparatus results in altered spectral properties of the sphingolipid precursor. *J. Cell Biol.* 113:1267–1279.

Paradiso, A.M., R.Y. Tsien, and T.E. Machen. 1984. Na+-H+ exchange in gastric glands as measured with a cytoplasmic-trapped, fluorescent pH indicator. *Proc. Natl. Acad. Sci. USA.* 81:7436–7440.

Ramotar, K., B. Boyd, G. Tyrrell, J. Gariepy, C. Lingwood, and J. Brunton. 1990. Characterization of Shiga-like toxin I B subunit purified from overproducing clones of the SLT-I B cistron. *Biochem. J.* 272:805–811.

Sandvig, K., O. Garred, K. Prydz, J.V. Kozlov, S.H. Hansen, and B. van Deurs. 1992. Retrograde transport of endocytosed Shiga toxin to the endoplasmic reticulum. *Nature (Lond.).* 358:510–512.

Seksek, O., J. Biwersi, and A.S. Verkman. 1995. Direct measurement of trans-Golgi pH in living cells and regulation by second messengers. *J. Biol. Chem.* 270:4967–4970.

Serafini, T., G. Stenbeck, A. Brecht, F. Lottspeich, L. Orci, J.E. Rothman, and F.T. Wieland. 1991. A coat subunit of Golgi-derived non-clathrin-coated vesicles with homology to the clathrin-coated vesicle coat protein β-adaptin. *Nature (Lond.).* 349:215–220.

Tartakoff, A.M. 1983*a*. Perturbation of vesicular traffic with the carboxylic ionophore monensin. *Cell.* 32:1026–1028.

Tartakoff, A.M. 1983*b*. Perturbation of the structure and function of the Golgi complex by monovalent carboxylic ionophores. *Methods Enzymol.* 98:47–59.

Tartakoff, A.M., and P. Vassalli. 1983. Lectin-binding sites as markers of Golgi subcompartments: proximal-to-distal maturation of oligosaccharides. *J. Cell Biol.* 97:1243–1248.

Tesh, V.L., and A.D. O'Brien. 1991. The pathogenic mechanisms of Shiga toxin and the Shiga-like toxins. *Mol. Microbiol.* 5:1817–1822.

Thastrup, O., P.J. Cullen, B.K. Drobak, M.R. Hanley, and A.P. Dawson. 1990. Thapsigargin, a tumor promoter, discharges intracellular Ca^{2+} stores by specific inhibition of the endoplasmic reticulum $Ca^{2(+)}$-ATPase. *Proc. Natl. Acad. Sci. USA.* 87:2466–2470.

Turner, J.R., and A.M. Tartakoff. 1989. The response of the Golgi complex to microtubule alterations: the roles of metabolic energy and membrane traffic in Golgi complex organization. *J. Cell Biol.* 109:2081–2088.

Tycko, B., and F.R. Maxfield. 1982. Rapid acidification of endocytic vesicles containing α 2-macroglobulin. *Cell.* 28:643–651.

Velasco, A., L. Hendricks, K.W. Moremen, D.R. Tulsiani, O. Touster, and M.G. Farquhar. 1993. Cell type-dependent variations in the subcellular distribution of alpha-mannosidase I and II. *J. Cell Biol.* 122:39–51.

Wood, S.A., J.E. Park, and W.J. Brown. 1991. Brefeldin A causes a microtubule-mediated fusion of the trans-Golgi network and early endosomes. *Cell.* 67:591–600.

Yamashiro, D.J., S.R. Fluss, and F.R. Maxfield. 1983. Acidification of endocytic vesicles by an ATP-dependent proton pump. *J. Cell Biol.* 97:929–934.

Yilla, M., A. Tan, K. Ito, K. Miwa, and H.L. Ploegh. 1993. Involvement of the vacuolar H(+)-ATPases in the secretory pathway of HepG2 cells. *J. Biol. Chem.* 268:19092–19100.